SUPPLEMENTAL MATERIAL

Cross-over between athermal jamming and the thermal glass transition

M. Dinkgreve[1] , M.A.J. Michels[2], T. G. Mason[3] and D. Bonn[1]

[1]*Institute of Physics, University of Amsterdam, Science Park 904, 1018 XH Amsterdam, The Netherlands*
[2]*Department of Applied Physics, Eindhoven University of Technology, P.O. Box 513, 5600 MB Eindhoven, The Netherlands*
[3]*Departments of Physics and Astronomy and Chemistry and Biochemistry, University of California Los Angeles, CA 90095, USA*

1. Characteristic material properties

TABLE S1. All parameters used in this work for the different systems at T=25°C. R is the particle radius, Σ the surface tension, ϵ the interaction energy of the particles, σ_0 the athermal stress scale, σ_T the thermal stress scale, and η_0 a prefactor of the order of the viscosity of the suspending phase.

	PMMA [1]	Emulsion 250nm [2]	Emulsion 530nm [2]	Emulsion 740nm [2]	Emulsion mobile	Emulsion rigid	Emulsion soft
R [m]	1.83E-7	2.50E-7	5.30E-7	7.40E-7	1.6E-6	1.6E-6	1.6E-6
Σ [N/m]	-	9.80E-3	9.80E-3	9.80E-3	1.50E-3	3.60E-3	1.40E-3
ϵ/k_BT	-	1.51E+5	6.78E+5	1.32E+6	9.46E+5	2.27E+6	8.83E+5
$\sigma_0 = \Sigma/R$ [Pa]	-	3.92E+4	1.85E+4	1.32E+4	9.38E+2	2.25E+3	8.75E+2
$\sigma_T = \alpha k_BT/R^3$ [Pa]	2.90E+3	9.10E+3	9.55E+2	3.51E+2	3.47E+1	3.47E+1	3.47E+1
η_0 [Pa s]	1E-3	1E-3	1E-3	1E-3	1E-3	1E-3	1E-3

2. Thermal systems with 740 nm emulsion included

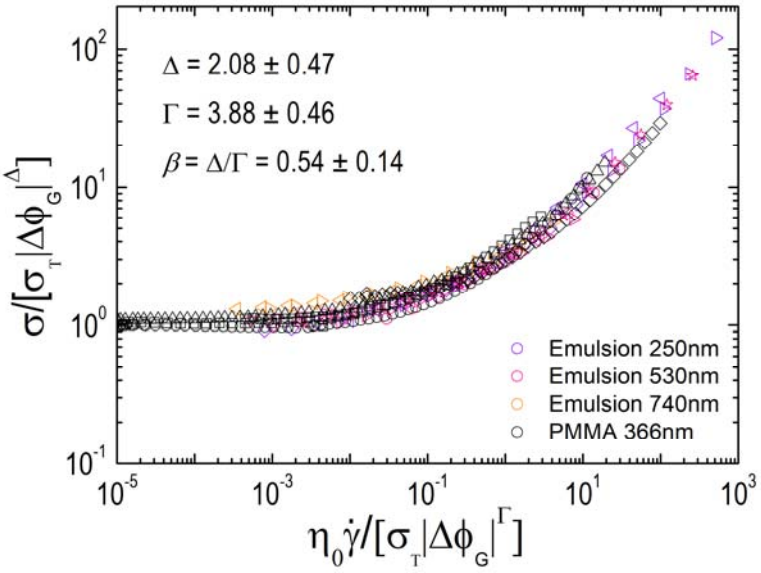

Figure S1: Rescaling the flow curves for thermal systems for $\varphi_G < \varphi < \varphi_J$ (cf. Figure 2(b)), with the 740nm emulsion.

3. Average and spread of the exponent values

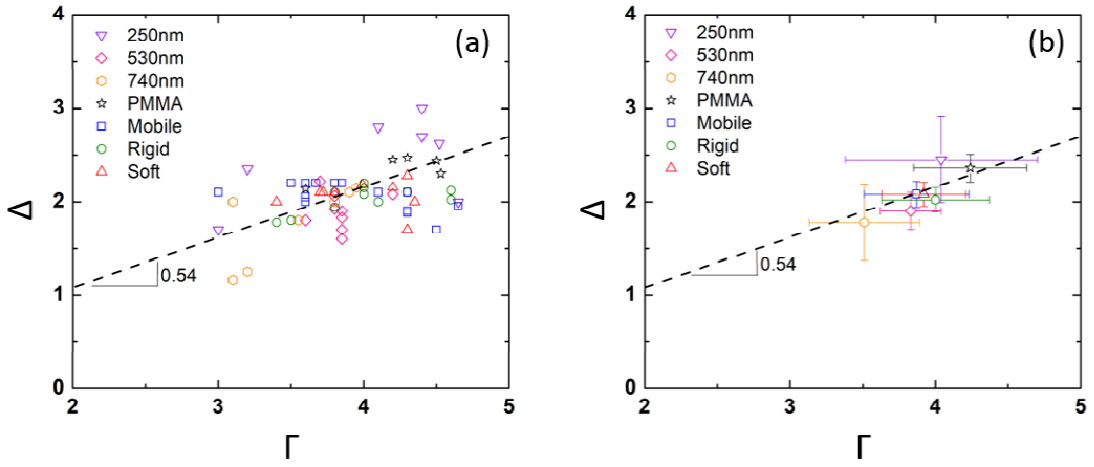

Figure S2: (a) Δ versus Γ for the different systems and volume fractions. (b) Average Δ and Γ per system with corresponding standard deviation.

4. Range of volume fractions

Figure S3 shows the flow curves of all the thermal and athermal systems that are studied. The corresponding volume fractions per system are given below. The volume fractions reported for the emulsion systems *R*=250, 530, and 740 nm are effective volume fractions that are corrected for screened electrostatic repulsions between droplet surfaces [2], not bare droplet (i.e. oil) volume fractions.

Mobile emulsion: 0.8, 0.78, 0.76, 0.74, 0.72, 0.7, 0.68, 0.67, 0.66, 0.64, 0.63, 0.62, 0.61, 0.6, 0.59, 0.58, 0.57, 0.56, 0.55, 0.5, 0.45, 0.4, 0.35, 0.25, 0.2, 0.1
Rigid emulsion: 0.8, 0.76, 0.72, 0.7, 0.68, 0.66, 0.65, 0.63, 0.6, 0.5, 0.4, 0.3
Soft emulsion: 0.8, 0.76, 0.72, 0.7, 0.68, 0.66, 0.65, 0.63, 0.6, 0.55, 0.5, 0.4, 0.3
Emulsion R=250nm: 0.87, 0.81, 0.72, 0.65, 0.63, 0.6, 0.58
Emulsion R=530nm: 0.72, 0.68, 0.66, 0.64, 0.63, 0.62, 0.61, 0.60, 0.69
Emulsion R=740nm: 0.74, 0.72, 0.7, 0.68, 0.66, 0.64, 0.62
PMMA: 0.63, 0.62, 0.6, 0.59, 0.58

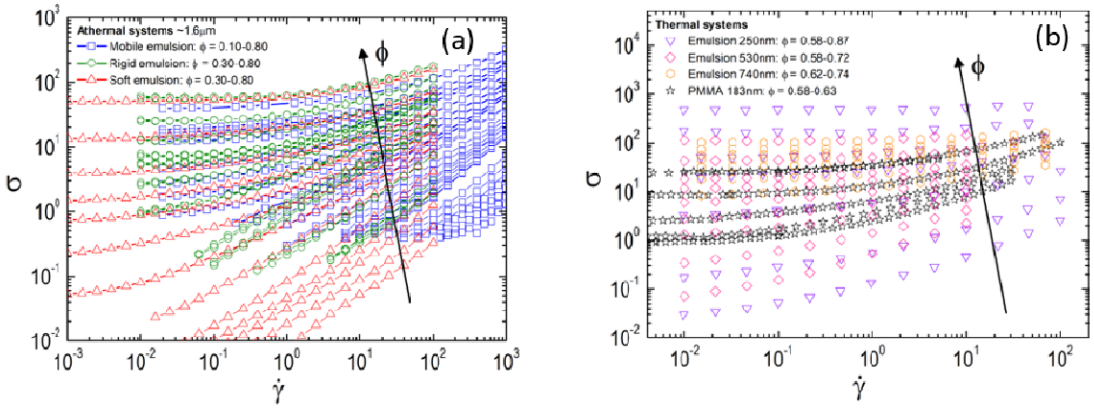

Figure S3: (a) Flow curves of athermal castor oil-in-water emulsions with different interactions and different

volume fractions (from bottom to top with increasing ϕ). (b) Flow curves of thermal systems: different droplet sizes of silicone oil-in-water emulsions and PMMA particles (from bottom to top with increasing ϕ).

5. Extension of the jamming model to thermal glassy behavior

The microscopic model in [3, 4] of heterogeneous dynamics and jamming assumes the existence of two characteristic microscopic rates, or inverse timescales. The first rate is the typical rate for single-particle mobility under shear, i.e., the average inverse time for contacting particles to get separated - under a standard unit shear stress - by a distance of the order of their own diameter; this average microscopic rate is directly proportional to the inverse of the macroscopic viscosity η and will be denoted $1/\tau_\eta$. For jammed particles this rate is zero, so in the context of our two-state model this rate is, apart from a factor of order unity, equal to the rate of the mobile fraction. In the high-temperature/low-Péclet limit, where thermal effects drive random particle motion, τ_η is - by virtue of the Fluctuation-Dissipation Theorem - equal to the cage-escape time τ_α of thermal equilibrium. In the low-temperature/high-Péclet limit that theorem does not apply and in equilibrium the particles do not move; both the affine and the disordered nonaffine motion are only driven by shear, and the timescale τ_η for the dissipative response to shear still exists. The second timescale, τ_{het} is the lifetime of the fluctuating pattern of stagnant and mobile regimes. Both time scales increase and become widely separated when the stagnant fraction increases, with $\tau_{het} \gg \tau_\eta$. Like in second-order critical transitions the characteristic length scale ξ of the heterogeneous domains diverges as a power-law in approach of the yield-stress line and becomes the dominant variable. All the other variables then have again a power-law dependence on ξ:

$$\frac{\xi(s)}{\xi(0)} = \left[\frac{\tau_\eta(s)}{\tau_\eta(0)}\right]^{\nu/m} = \left[\frac{\tau_{het}(s)}{\tau_{het}(0)}\right]^{\nu/n} = \left|1 - \frac{s}{s_c}\right|^{-\nu} \qquad \text{(S.1)}$$

with $n > m$. Here s is the fraction of particles arrested in cages, and s_c the critical fraction where macroscopic flow halts. The viscosity $\eta = \sigma/\dot{\gamma}$ is proportional to τ_η and hence the macroscopic rheology follows similarly:

$$\eta(s) = \eta(0)|1 - s/s_c|^{-m} \qquad \text{(S.2)}$$

The stress-dependent steady-state value of s follows from a balance between stress-induced cage escape and arrest through free-volume fluctuations. The average cage-escape rate can then be equated to the decay rate of the heterogeneity patterns; the escape rate contains two terms and is dominated by whichever is the fastest:

$$s\left[\frac{1}{\tau_b} f\left(\sigma/\sigma_y\right) + \dot{\gamma}\right] = \frac{1}{\tau_{het}(s)} \qquad \text{(S.3)}$$

The two terms between square brackets cover two extreme cases, the static and collective-flow limits, respectively. The first term represents the stress-induced escape of a stagnant particle from the static cage of particles surrounding it, the second term represents the case where the cage itself is flowing with the particle. The first term $1/\tau_b = \sigma_y/\eta_N = \left(\sigma_0/\eta_0\right)|\Delta\varphi|^{\Delta+M}$ is a characteristic rate for barrier crossing, with $\sigma_y = \sigma_0|\Delta\varphi|^{\Delta}$ the yield stress and $\eta_N = \eta_0|\Delta\varphi|^{-M}$ the Newtonian viscosity.

Below σ_y no cage escape is possible, so $1/\tau_b$ has to be multiplied by a function $f\left(\sigma/\sigma_y\right)$ that is zero if its argument is below unity. Above σ_y the probability of barrier crossing rapidly increases, so above unity $f\left(\sigma/\sigma_y\right)$ will be a steeply increasing function of its argument.

Crossover to collective shear-thinning flow of all particles takes over when the typical rate for barrier crossing, $1/\tau_b$, becomes of the order of the average rate, i.e. equal to the second term between square brackets; so the crossover rate $\dot{\gamma}_{co}$ equals $1/\tau_b = (\sigma_0/\eta_0)|\Delta\varphi|^{\Gamma}$, with $\Delta + M = \Gamma$.

At this crossover point the excess (viscous) stress $\sigma - \sigma_y$ becomes of the order of the elastic stress, i.e. of order σ_y, so $f(2)$ can be chosen of order unity. For still higher stresses $f(\sigma/\sigma_y)$ saturates around that level and the first term between square brackets becomes irrelevant. So typically $f(x) = 0$ when $x < 1$, $f(x) = (x-1)^p$ when $1 < x < 2$ and $f(x) = 1$ when $x \geq 2$.

In [3,4] we show how the solution of the above balance equation for *s* at given stress or rate leads to the correct asymptotic high- and low-rate forms of the Herschel-Bulkley and Cross equations, and their merging at high rates. The macroscopic exponents are found to follow from the microscopic ones through the identification $m \equiv M = \Gamma - \Delta$ and $n \equiv \Gamma$. Moreover we there derive from a scaling of free-volume fluctuations that $\Delta \equiv n - m = d\nu$, with d the (possibly fractal) dimension of the heterogeneous domains; in the literature a correlation-length exponent $\nu \cong 0.7$ is more than once reported, this would lead to $\Delta \cong 2.1$ in case $d = 3$ (see [3,4] and references therein).

If we postulate that the above microscopic mechanisms of heterogeneous dynamics and critical behavior applies both to the glass and the jamming transition, with the same critical exponents, we only need to choose in each case the appropriate characteristic stress (σ_0 or σ_T), characteristic inverse timescale (σ_0/η_0 or σ_T/η_0), and relevant critical volume fraction (φ_G or φ_J). When considering the two transitions simultaneously it is logical to take the barrier stress for cage escape σ_y as the sum of both the random thermal stress and the enthalpic deformational stress. Accordingly in rescaling the experimental stress data one should then use the additive yield stresses as the scale factor:

$$\sigma_{co} = \sigma_T|\Delta\varphi_G|^{\Delta} + \sigma_0\left|\Delta\varphi_J\right|^{\Delta} \qquad \text{(S.4)}$$

To rescale the experimental flow rates one should then similarly use the added crossover rates of the glass and jamming cases:

$$\dot{\gamma}_{co} = (\sigma_T/\eta_0)|\Delta\varphi_G|^{\Gamma} + (\sigma_0/\eta_0)\left|\Delta\varphi_J\right|^{\Gamma} \qquad \text{(S.5)}$$

However, the above combined treatment of the glass and jamming transitions supposes that these transitions are sufficiently separated in terms of the crossover rates, with a Newtonian regime at high rates in approach of the jamming concentration. As seen in the main text, the data for the thermal emulsions do not show this second regime of a diverging viscosity; apparently the separation is insufficient. To suppress in the data collapse the influence of the approaching jamming concentration on the thermal data below ϕ_J we have to multiply in (S.4) and (S.5) the factor σ_0 with a step function $\theta = 0$ if $\phi < \phi_J$ and $R < 1\mu$m and unity otherwise.

6. References

[1] G. Petekidis, D. Vlassopoulos, and P. N. Pusey, Journal of Physics: Condensed Matter **16**, S3955 (2004)

[2] T. Mason, J. Bibette, and D. A. Weitz, Journal of Colloid and Interface Science **179**, 439 (1996)

[3] J. Paredes, M. A. J. Michels, and D. Bonn, Physical Review Letters **111**, 015701 (2013)

[4] M. Dinkgreve, J. Paredes, M. A. J. Michels, and D. Bonn, Physical Review E **92**, 012305 (2015)